Toll-like Receptor 2 and Mitogen- and Stress-activated Kinase 1 Are Effectors of *Mycobacterium avium*-induced Cyclooxygenase-2 Expression in Macrophages*

Sushil Kumar Pathak‡, Asima Bhattacharyya, Shresh Pathak, Chaitali Basak, Debabrata Mandal, Manikuntala Kundu§, and Joyoti Basu§

From the Department of Chemistry, Bose Institute, 93/1 Acharya Prafulla Chandra Road, Calcutta 700009, India

Understanding how pathogenic mycobacteria subvert the protective immune response is crucial to the development of strategies aimed at controlling mycobacterial infections. Prostaglandin E_2 exerts an immunosuppressive function in the context of mycobacterial infection. Because cyclooxygenase-2 (COX-2) is a rate-limiting enzyme in prostaglandin biosynthesis, there is a need to delineate the mechanisms through which pathogenic mycobacteria regulate COX-2 expression in macrophages. Our studies demonstrate that the NF-κB and CRE elements of the COX-2 promoter are critical to *Mycobacterium avium*-induced COX-2 gene expression. *M. avium*-triggered signaling originates at the Toll-like receptor 2 (TLR2). Ras associates with TLR2 and activates the mitogen-activated protein kinase (MAPK) extracellular signal-regulated kinase (ERK), whereas tumor necrosis factor receptor-associated factor 6 (TRAF6)/transforming growth factor β-activated kinase 1 (TAK1)-dependent signaling activates p38 MAPK. Both ERK and p38 MAPK activation converge to regulate the activation of mitogen- and stress-activated kinase 1 (MSK1). MSK1 mediates the phosphorylation of the transcription factor CREB accounting for its stimulatory effect on CRE-dependent gene expression. *M. avium*-triggered cytoplasmic NF-κB activation following IκB phosphorylation is necessary but not sufficient for COX-2 promoter-driven gene expression. MSK1 activation is also essential for *M. avium*-triggered NF-κB-dependent gene expression, presumably mediating nucleosomal modifications. These studies demonstrate that the nuclear kinase MSK1 is necessary in regulating the pathogen-driven expression of a gene by controlling two transcription factors. The attenuation of MSK1 may therefore have potential benefit in restricting survival of pathogenic mycobacteria in macrophages.

To design novel therapeutics and to rationalize vaccination strategies against mycobacterial diseases, it is of foremost importance to understand the mechanisms by which mycobacteria subvert the protective immune response. The response of macrophages to invasion by intracellular pathogens such as mycobacteria depends on the signals triggered during the initial contact of the bacterium with the macrophages. Prostaglandin E_2 (PGE_2)[1] is believed to exert an immunosuppressive function in the context of mycobacterial infections. PGE_2 interferes with T lymphocyte responses by inhibiting the production of interleukin-2 (1). PGE_2 also inhibits the secretion of interferon-γ, which is important in activating T cells and macrophages (2). Cooper and colleagues (3) reported that the ability of the virulent *Mycobacterium avium* to attenuate macrophage activation was dependent on its ability to trigger p38 mitogen-activated protein kinase (MAPK)-dependent production of PGE_2. These observations were supported by a case report in which monocytes from a child with disseminated *M. avium* infection demonstrated a defect in bactericidal activity which could be offset by treatment with indomethacin (4). The critical role of PGE_2 is also supported by a report that human immunodeficiency virus envelope glycoprotein (gp120) can enhance *M. avium* replication within macrophages by induction of PGE_2 (5).

Cyclooxygenase-2 (COX-2) is a key enzyme catalyzing the rate-limiting step in the inducible production of prostaglandins. COX-2 catalyzes the conversion of arachidonic acid to PGH_2, which is then metabolized by terminal synthases to a variety of biologically active prostanoids (6). COX-2 gene expression is regulated at the level of transcription as well as post-transcriptionally. The regulation of the COX-2 promoter in macrophages is complex and involves different promoter elements. The transcriptional activation of the COX-2 gene depends on the stimulus-coupled binding of transcription factors (7), including NF-κB, C/EBPβ, and AP-1 (8–12). The CRE-element is the most generally required promoter element, being essential for both basal and induced COX-2 transcription in a variety of cell types (13–17). The specific factors regulating COX-2 induction depend on the cell type as well as on the stimulus.

Considering that COX-2 is likely to play a critical role in *M. avium*-triggered PGE_2 release from macrophages, we set out to explore the signaling cascades and the cis-regulatory elements governing COX-2 induction from *M. avium*-challenged macrophages. Our results demonstrate that TLR2-dependent ERK and p38 activation converge upon the activation of mitogen- and stress-activated kinase 1 (MSK1), which is

---

‡ Supported by a Junior Research Fellowship from the Council of Scientific and Industrial Research, Government of India.

§ To whom correspondence may be addressed. Tel.: 91-33-2350-6619; Fax: 91-33-2350-6790; E-mail: joyoti@vsnl.com (J. B.) or manikuntala@vsnl.net (M. K.).

[1] The abbreviations used are: PGE_2, prostaglandin E_2; COX-2, cyclooxygenase-2; ERK, extracellular signal-regulated kinase; MAPK, mitogen-activated protein kinase; TLR2, Toll-like receptor 2; MSK1, mitogen- and stress-activated kinase 1; PBS, phosphate-buffered saline; m.o.i., multiplicity of infection; CMV, cytomegalovirus; TBS, Tris-buffered saline; GST, glutathione *S*-transferase; LPS, lipopolysaccharide.

TABLE I
Primers used for mutation of transcription factor binding sites in the murine COX-2 promoter
Primers "b" and "c" are defined under "Experimental Procedures."

Mutation at the binding site for	Primer b	Primer c
NFκB	5′-GGGGAGAGGTGAGGGTTCCCTTAGTTAGGA -3′	5′- TCCTAACTAAGGGAACCCTCACCTCTCCCC-3′
C/EBPβ	5′- TGCCGCTGCGGTTCTGCCACTCACTGAAGCAGA-3′	5′-TCTGCTTCAGTGAGTGGCAGAACCGCAGCGGCA-3′
AP1	5′-AGCGGAAAGACAGAGCCACTACGTCACGTG -3′	5′- CACGTGACGTAGTGGCTCTGTCTTTCCGCT-3′
CREB	5′-AGACAGAGTCACCACTTCACGTGGAGTCCGCTT-3′	5′-AAGCGGACTCCACGTGAAGTGGTGACTCTGTCT-3′

instrumental in controlling both NF-κB- and CRE-driven transcription of the COX-2 gene. To the best of our knowledge, this is the first demonstration of the role of MSK1 in controlling pathogen-driven gene expression of COX-2, a molecule that plays a central role in pathogenesis.

EXPERIMENTAL PROCEDURES

U0126, SB203580, H89, and manumycin A were purchased from EMD Biosciences, San Diego, CA. Polymyxin B, CREBTIDE, anti-CREB and anti-FLAG-agarose were products of Sigma. Protease inhibitors were from Roche Applied Science. Antibodies to MSK1, p65, and p50 were purchased from Santa Cruz Biotechnology Inc. (Santa Cruz, CA). Antibodies specific for p38 MAPK, ERK, phospho-ERK, phospho-p38, phospho-CREB, and anti-Ras were from Cell Signaling Technology (Beverly, MA). Anti-TLR2 antibody was from Imgenex India (Bhubaneswar). [γ-^{32}P]ATP was from Jonaki, BRIT (Hyderabad, India).

Growth of M. avium—*M. avium* (NCTC 8562) was obtained from the All India Institute of Medical Sciences, New Delhi), grown in Middlebrook 7H9 broth (Difco, Detroit, MI) supplemented with oleic acid-albumin-dextrose supplement and 0.04% Tween 80 until mid-log phase, harvested, washed, and resuspended in a small volume of phosphate-buffered saline (PBS) containing 0.04% (v/v) Tween 80. The suspension was briefly sonicated until no bacterial clumps were visualized by microscopy. The preparation was diluted to a concentration of 2×10^8 colony-forming units/ml in 10% glycerol and stored in aliquots at −80 °C. Freshly thawed aliquots were used no more than once. Where indicated, cells were incubated with polymyxin B (10 μg/ml) for 30 min prior to use.

Cell culture—The murine macrophage cell line RAW264.7 was obtained from the National Centre for Cell Science, Pune, India, and cultured in Dulbecco's modified Eagle's medium supplemented with 10% fetal bovine serum, 2 mM glutamine, and antibiotics. Where indicated, RAW264.7 cells were challenged with *M. avium* at a multiplicity of infection (m.o.i.) of 2.

Plasmid constructs—Using genomic DNA from RAW264.7 cells as template, the COX-2 promoter region (−891 to +9) was amplified by PCR using the primer pair 5′-CGG**GGTACC**CAAACACTGTTTCT-GAAT-3′ (sense, primer a) and 5′-ATA**AAGCTT**TTTGACAACTGGCT-GCTA-3′ (antisense, primer b). The resulting COX-2 promoter region was cloned into the vector pGL2 Basic (Promega) harboring the promoter-less luciferase gene, using asymmetric KpnI and Hind III sites (underlined) to generate the plasmid pCOX301. NF-κB(−402/−392), C/EBPβ(−135/−130), AP-1(−65/−60), or CRE(−60/−56) binding sites were mutated by deleting the underlined bases from the respective sites as indicated: 5′-GGG**GA**TTCC-3′ (for NF-κB), 5′-TC**TT**GC**GC**A**A**-3′ (for C/EBPβ), 5′-ACAGAG**TCA**C-3′ (for AP1) and 5′-CACT**ACG**TCA-3′ (for CRE). Mutants were generated by overlap extension PCR. The primers used are depicted in Table I. The initial rounds of PCR were carried out using the primer pairs a and b for one reaction, c and d for the second reaction, and pCOX301 as template. The products of each PCR were purified and used as templates for the second round of PCR using the primers a and d. The final products were cloned between the KpnI and HindIII sites of pGL2 Basic. Vectors for wild type and dominant-negative Ras (Ras S17N); wild type and dominant-negative (S32A, S36A) IκBα in pCMV were purchased from BD Biosciences. For generating FLAG-tagged Ras expression vectors, the respective genes were excised from the parent vectors described above using EcoRI and BamHI and cloned between the EcoRI and BamHI sites in pFLAG-CMV6c. Wild type and dominant-negative (amino acid residues 289–522) TRAF6 in pRK-FLAG were gifts from Tularik Inc. Wild type and dominant-negative (K63W) HA-TAK1 were gifts from Dr. Kuni Matsumoto, Nagoya University, Japan; wild type and dominant-negative (D195A) MSK1 in pCMV-FLAG were gifts from Dr. Dario Alessi, University of Dundee, UK. Wild type TLR4 (mTLR4) in pEF-Bos was a gift from Dr. Yoshinori Nagai of the University of Tokyo, Japan. Dominant-negative mTLR4
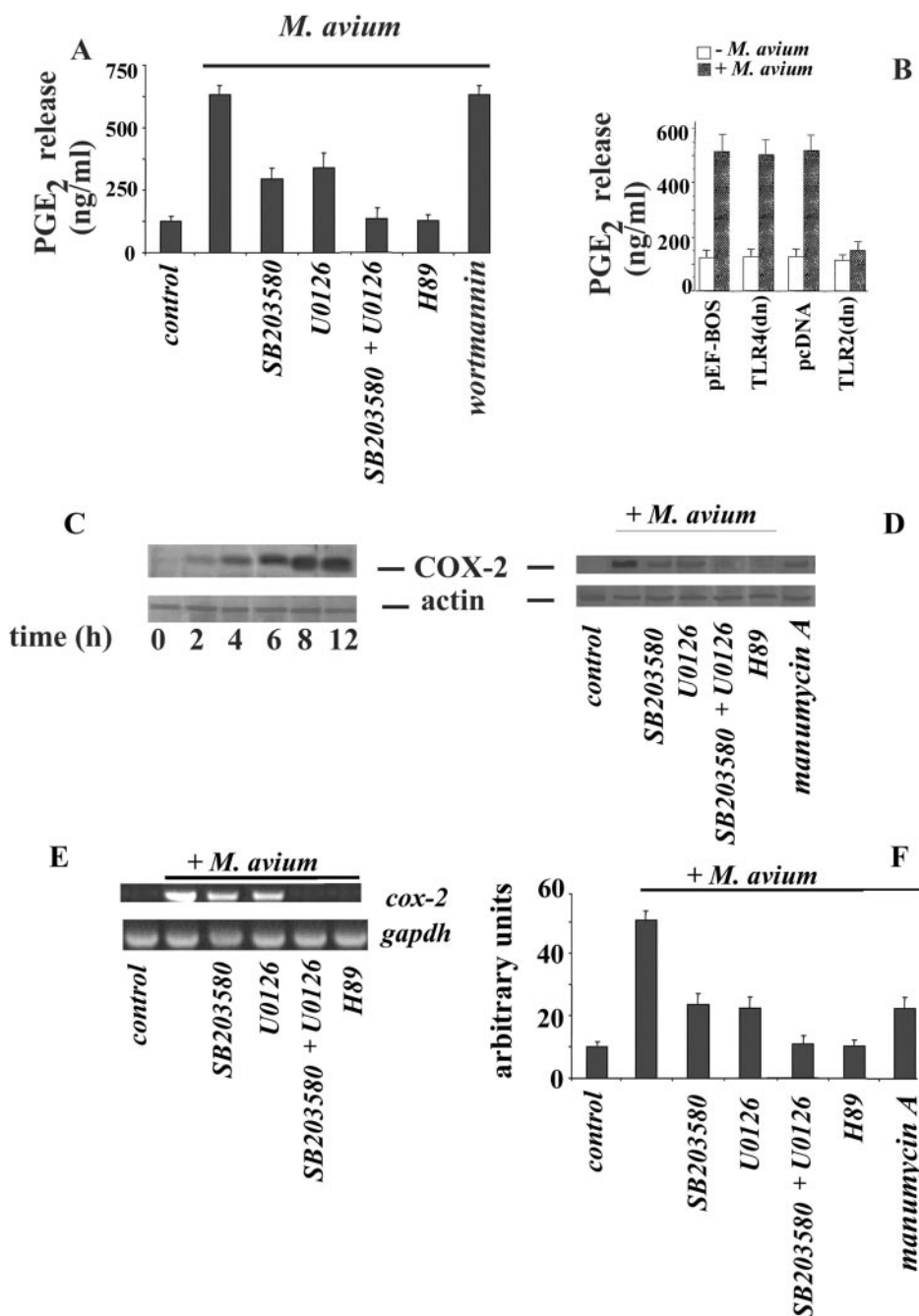
(P712H) was generated by site-directed mutagenesis based on the principle of overlap extension PCR. Using pEF-BOS-TLR4 as template, the first round of PCR was performed with primer pairs a and b for one reaction and primer pairs c and d for the second reaction. The second round of PCR was performed using the products of the first round as templates, and primers a and d. Primers a, b, c, and d were 5′-ACAG-AATTCTCAGCGTTCTTATCCCTT-3′, 5′-GACTTTATTCATGGTGTA-GCC-3′, 5′-GGCTACACCATGAATAAAGTC-3′, and 5′-CGCGGATCC-GGTCCAAGTTGCCGTTTC-3′, respectively. The resulting 1.2-kb PCR product was cloned in pUC19 between the EcoRI and BamHI sites, sequenced on both strands, and an Xho-BamHI (468 bp) fragment containing the mutated TLR4 gene encoding amino acid residues 679–835 was then excised and used to replace the Xho-BamHI fragment of wild type TLR4 in pEF-BOS. p4NF-κB-luc containing four NF-κB sites in tandem fused to the luciferase reporter gene, was a gift from Dr. A. Brent Carter of the University of Iowa. The p6CRE-luc construct containing 6 CRE sites in tandem fused to the luciferase reporter gene was a gift from Dr. Steve Rees of GlaxoSmithKline. pGEX/Raf-RBD was a gift from Dr. Robert J. Sheaff of the University of Minnesota. cDNA products for murine TLR2 and CREB were obtained by reverse transcription-PCR from a total RNA preparation from RAW264.7 cells using the primer pairs: 5′-CTAGCTAGCTAGATGCTACGAGCTCTT-3′ (sense) and 5′-CCGCTCGAGCGGCTAGGCCTTTATTGC-3′ (antisense) for TLR2; and 5′-ATAAAGCTTATGGAATCTGGA-3′ (sense) and 5′-A-TGGATCCATCTGATTTGTGGCAGTA-3′ (antisense) for CREB. The resulting PCR products were cloned in pcDNA3.1 (between NheI and XhoI sites) for TLR2 and pFLAG-CMV-6a (between HindIII and BamHI sites) for CREB. For generating dominant-negative dominant TLR2 (carrying a 13-amino acid deletion from the C terminus), a 2313-bp fragment was amplified by PCR using the sense primer mentioned above and the antisense primer: 5′-CCGCTCGAGCGGCTGGCCT-TCATC-3′. The resulting PCR product was cloned in pcDNA 3.1 between NheI and XhoI sites. Site-directed mutagenesis was performed to generate dominant-negative CREB (S133A). Primers b and c were 5′-AGGAGGCCTGCCTACAGGAAA-3′ and 5′-TTTCCTGTAGGCAG-GCCTCCT-3′, respectively. All constructs were checked by sequencing on both strands.

Enzyme Immunoassay for PGE$_2$—Supernatants from mock-treated and *M. avium*-treated macrophages were harvested at the indicated times and tested for the presence of PGE$_2$ using the BIOTRAK PGE$_2$ assay kit from Amersham Biosciences.

Western Blotting—Proteins were separated by SDS-PAGE and then transferred electrophoretically to polyvinylidene difluoride membranes. The blots were blocked with 5% nonfat dry milk in Tris-buffered saline (TBS) for 1 h at room temperature and subsequently incubated overnight at 4 °C with primary antibodies in TBS-Tween 20 (1%, v/v) (TBST) with 5% (w/v) bovine serum albumin. Following three washes of 5 min each with TBST, the blots were incubated with horse radish peroxidase-conjugated goat anti-rabbit IgG (Santa Cruz Biotechnology, Inc.) (or appropriate secondary antibodies) in blocking buffer for 1 h at room temperature. After three washes with TBST, the blots were developed by chemiluminescence using the Phototope-HRP Western blot detection kit (Cell Signaling Technology) and exposed to x-ray film (Kodak XAR5).

RNA Isolation and Reverse Transcription-PCR—Total RNA was prepared from cells using the RNeasy Mini kit (Qiagen) according to the manufacturer's protocol. 100 ng of RNA was reverse-transcribed using the Titan 1-tube reverse transcription-PCR Kit (Roche Applied Sciences). The sense primer 5′-GGGGTTGCTGGGGGAAATGTG-3′, and the antisense primer 5′-GGTGGCTGTTTTGGTAGGTG-3′, were used to amplify 479 bp of COX-2 mRNA. Glyceraldehyde-3-phosphate dehydrogenase was amplified using the primers: 5′-CCA TCA ATG ACC CCT TCA TTG ACC-3′ (sense), and 5′-GAA GGC CAT GCC AGT GAG CTT CC-3′ (antisense) to generate a 604-bp product. The PCR conditions for COX-2 mRNA were denaturation at 94 °C for 30 s, annealing at 50 °C for 1 min, and extension at 68 °C or 1 min for 35 cycles.

FIG. 1. ***M. avium* stimulates PGE$_2$ release and COX-2 expression in RAW264. 7 cells.** *A*, 2×10^5 cells were treated with *M. avium* for 8 h, and the culture medium was collected and assayed for the release of PGE$_2$ using the BIOTRAK PGE$_2$ ELISA kit according to the manufacturer's protocol. Where indicated, cells were left untreated or treated with U0126 (15 μM) or SB203580 (5 μM) or wortmannin (200 nM), or a combination of U0126 and SB203580 at the same concentrations, or H89 (10 μM), for 30 min followed by the treatment with *M. avium* at an m.o.i. of 2 for 8 h. The released PGE$_2$ was measured as described. *B*, RAW264.7 cells were transfected with empty vector (pcDNA3.1 or pEF-BOS) or with dominant-negative(*dn*)-TLR4 [TLR4(P712H)] or -TLR2, followed by treatment with *M. avium* at an m.o.i. of 2 for 8 h. PGE$_2$ release was subsequently assayed. Results shown represent the means ± S.D. of three independent experiments. *C*, 5×10^5 cells were seeded in a 24-well plate, treated with *M. avium* at an m.o.i. of 2 for different periods of time periods as indicated, washed, and lysed. The expression of COX-2 in the lysates was analyzed by Western blotting using anti-COX-2 antibody. The blot is representative of the results obtained in three independent experiments. *D*, cells were left untreated or treated with U0126 (15 μM) or SB203580 (5 μM) or manumycin A (10 μM) or a combination of U0126 and SB203580 at the same concentrations, or H89 (10 μM) for 30 min followed by the treatment with *M. avium* at an m.o.i. of 2 for 8 h. Expression of COX-2 was analyzed as described in *panel C*. The blot is representative of results obtained in three independent experiments; *panel F* represents the results obtained from densitometric scanning of these gels (means ± S.D.). *E*, cells were left untreated or pretreated with the inhibitors SB203580 (5 μM) or U0126 (15 μM) or a combination of U0126 and SB203580 at the same concentrations, or H89 (10 μM) for 30 min followed by the treatment with *M. avium* at an m.o.i. of 2 for 6 h. Total RNA was isolated and reverse transcription-PCR was performed using primers specific for the COX-2 or the glyceraldehyde-3-phosphate dehydrogenase (*gapdh*) genes. The products were visualized on agarose gels by ethidium bromide staining. The data shown are representative of results obtained from three independent experiments.

Electrophoretic Mobility Shift Assay—To prepare nuclear extracts, plates with adhered cells were washed twice with ice-cold PBS and scraped in ice-cold TNE buffer (40 mM Tris HCl, pH 7.5, 0.1 M NaCl, 1 mM EDTA). Cells were pelleted at $600 \times g$ for 1 min, and pellets were resuspended in 400 μl of lysis buffer (10 mM HEPES, pH 7.9, 10 mM KCl, 0.1 mM EDTA, 0.1 mM EGTA, 1 mM dithiothreitol, 0.5 mM Pefabloc, 2 μg/ml leupeptin, 2 μg/ml aprotinin, 0.5 mg/ml benzamidine). Cells were lysed by the addition of 23 μl of 10% (v/v) Nonidet P-40 (Nonidet P-40) and the nuclear pellet was suspended in 25 μl of ice-cold extraction buffer (20 mM HEPES, pH 7.9, 0.4 M NaCl, 1 mM EDTA, 1 mM EGTA, 1 mM dithiothreitol, 0.5 mM Pefabloc, 2 μg/ml leupeptin, 2 μg/ml aprotinin, 0.5 mg/ml benzamidine), kept on ice for 30 min with occasional mixing, and centrifuged at $10, 000 \times g$ for 5 min at 4 °C. The supernatant (nuclear extract) was immediately frozen and stored at -70 °C. Typically, 15 μg of nuclear extract was incubated on ice for 5 min in the absence or presence of competitor DNA in a volume of 20 μl containing 4 μl of 5× binding buffer (125 mM HEPES, pH 8, 2.5 mM EDTA, 2.5 mM dithiothreitol, 5% Nonidet P-40, 250 mM NaCl, 20% (v/v) glycerol), and 0.75 μg of poly(dI-dC) as nonspecific competitor DNA. The ^{32}P-end-labeled double-stranded oligonucleotides (60,000 cpm per reac-

tion) containing the COX-2 gene-specific NF-κB binding site (5′-GGT-GAGGGG**GA**TTCCCTTAGTTA-3′) (or the mutated oligonucleotide with the sites of mutation (GA → CC) in boldface) or the COX-2-specific CRE site (5′-GTCACCACT**ACG**TCACGTGGAG-3′) (or the mutated oligonucleotide with the sites of mutation (ACG → GAT) in boldface) was added, and the mixture was incubated for 30 min at 25 °C. The DNA-protein complex formed was separated from the oligonucleotide on a 4% native polyacrylamide gel. The gel was dried and analyzed by autoradiography. For supershift assays, nuclear extracts were incubated for 30 min at 25 °C with rabbit polyclonal antibodies against p50, p65 (for NF-κB), or CREB (for CRE) or no antibody before incubation with the radiolabeled probe.

Luciferase reporter assays—Cells were transfected with luciferase reporter plasmid. Transfected cells were challenged with *M. avium*, washed once with PBS, and scraped into luciferase lysis buffer (50 mM Tris, pH 8, 70 mM K$_2$HPO$_4$, 0.1% Nonidet P-40, 2 mM MgCl$_2$, 1 mM dithiothreitol, 20 μg/ml aprotinin, 10 μg/ml pepstatin, 10 μg/ml leupeptin). The lysates were rapidly mixed, and insoluble material was pelleted by centrifugation at 4 °C. The supernatant was removed and stored at -80 °C. For promoter activation analysis, luciferase activity
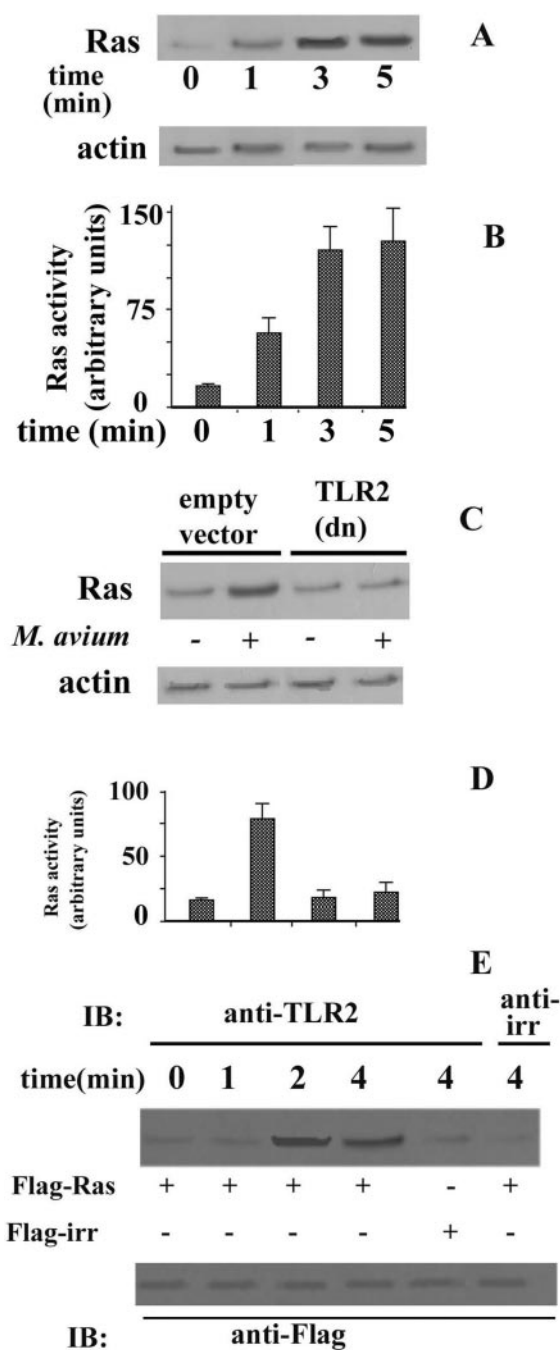
FIG. 2. *M. avium* **activates Ras in RAW264.7 cells in a TLR2-dependent manner.** RAW264.7 cells were challenged with *M. avium* for different periods of time as indicated and lysed, and lysates were incubated with 5 μg of GST-Raf-1 RBD immobilized on glutathione-Sepharose at 4 °C for 3 h. Bound Ras proteins were solubilized in Laemmli buffer and detected by SDS-PAGE and Western blotting using anti-Ras antibody. *Panel A* is a representative blot. *Panel B* represents the results from densitometric scans of the blots from three independent experiments (means ± S.D.). *C*, cells were transfected with either empty vector (pcDNA3.1) or dominant-negative TLR2 (*TLR2 (dn)*), then left untreated or treated with *M. avium* at an m.o.i. of 2 for 4 min. Cell lysates were prepared, and Ras activity was measured as described. The blot shown is representative of results obtained in three independent experiments. *D*, the densitometric scan of three independent experiments (means ± S.D.). For *panels A* and *C*, actin immunoblots indicate equal loading in all lanes. *E*, RAW264.7 cells were transfected with FLAG-tagged Ras (*Flag-Ras*) or an irrelevant FLAG-tagged construct (*Flag-irr*) and treated with *M. avium* for the indicated time periods. Cell extracts were immunoprecipitated with anti-FLAG agarose and then immunoblotted with anti-TLR2 antibody or irrelevant antibody (*anti-irr*). The *bottom panel* was obtained by immunoblotting with anti-FLAG. The blots are representative of results obtained in three independent experiments.

assays were performed in a luminometer, and the results were normalized for transfection efficiencies by assay of β-galactosidase activity.

Ras Activity Assay—Ras activity was measured by assaying for Ras proteins bound to the Ras-binding domain of Raf-1 expressed as a GST fusion protein (18). Briefly, cells (2×10^6) after treatment were washed with ice-cold PBS, lysed in lysis buffer (25 mM HEPES, pH 7.5, 150 mM NaCl, 10 mM MgCl$_2$, 5 mM EDTA, 25 mM NaF, 1 mM sodium orthovanadate, 10% glycerol, 10 μg/ml aprotinin, and 10 μg/ml leupeptin) and centrifuged. Lysate was incubated with 5 μg of Ras-binding domain of Raf-1 (Raf-1 RBD) at 4 °C for 3 h with gentle agitation, and the beads were washed thrice in lysis buffer. Bound Ras proteins were solubilized in Laemmli buffer and detected by SDS-PAGE followed by Western blotting using anti-Ras antibody.

Co-immunoprecipitation of Ras with TLR2—RAW 264.7 cells were transfected with FLAG-Ras expressing vector and challenged with *M. avium* for the indicated time periods. The cells were harvested, lysed in lysis buffer (40 mM Tris-HCl (pH 8.0), 500 mM NaCl, 0.1% Nonidet P-40, 6 mM EGTA, 10 mM sodium β-glycerophosphate, 10 mM NaF, 300 μM sodium orthovanadate, 2 mM phenylmethylsulfonyl fluoride, 10 μg/ml aprotinin, 1 μg/ml leupeptin, and 1 mM dithiothreitol), and centrifuged. The supernatant was then immunoprecipitated with anti-FLAG-agarose. The immunoprecipitated beads were washed three times with lysis buffer. The samples were fractionated on 15% SDS-polyacrylamide gels, transferred to a polyvinylidene difluoride membrane, and subjected to immunoblot analysis with antibodies specific for TLR2.

MSK1 Assay—Cells were washed with ice-cold PBS and lysed in lysis buffer containing 50 mM Tris-HCl, pH 7.5, 1 mM EDTA, 1 mM EGTA, 1 mM sodium orthovanadate, 1% (v/v) Triton X-100, 50 mM NaF, 5 mM sodium pyrophosphate, 0.27 M sucrose, 0.1%(v/v) β-mercaptoethanol, 1 mM benzamidine, 2 μg/ml leupeptin, and 0.2 mM Pefabloc. Lysates were clarified by centrifugation (5 min, 10,000 $\times$ g, 4 °C). MSK1 was immunoprecipitated by incubation with anti-MSK1 antibody. The immunoprecipitates were washed three times with lysis buffer and twice with kinase buffer (50 mM Tris-HCl, pH 7.4, 10 mM MgCl$_2$, 0.1 mM EGTA, 10 mM NaF, and 0.1% (v/v) β-mercaptoethanol). Beads were resuspended in 50 μl of kinase buffer containing 30 μM substrate peptide: EILSR-RPSYRK (CREBTIDE) and 0.1 mM [γ-^{32}P]ATP (20,0000 cpm/pmol). After incubation at 30 °C for 30 min, the incorporation of phosphates in CREBTIDE was determined using p81 phosphocellulose paper (19).

RESULTS

M. avium Stimulates PGE$_2$ Release from RAW264.7 Macrophages—Considering that PGE$_2$ release is one of the mechanisms used by virulent *M. avium* to down-regulate macrophage activation (3), we sought to investigate the mechanisms of *M. avium*-stimulated PGE$_2$ release from RAW264.7 macrophages. The levels of PGE$_2$ released from RAW264.7 cells were measured using an enzyme-linked immunosorbent assay. Challenge of macrophages with *M. avium* for 8 h induced a rise in PGE$_2$ levels (Fig. 1*A*). Members of the TLR protein family are key regulators of innate immune activation induced by pathogenic mycobacteria (20). *M. avium* signals in macrophages through TLR2 (21). Consistent with a role of TLR2-dependent signaling in *M. avium*-stimulated PGE$_2$ release, transfection of RAW264.7 cells with dominant-negative TLR2, led to abrogation of PGE$_2$ release following *M. avium* challenge (Fig. 1*B*). On the other hand, cells transfected with dominant-negative TLR4 (TLR4 harboring the mutation P712H) still showed release of PGE$_2$ when challenged with *M. avium*. In results described in Fig. 5, we have validated that TLR4(P712H) does function as a dominant-negative in the present context. TLR4 therefore did not appear to play any role in *M. avium*-mediated PGE$_2$ release.

M. avium-stimulated PGE$_2$ Release Depends on the ERK and p38 MAPKs—PGE$_2$ release from *M. avium*-challenged cells was inhibited when cells were pretreated with pharmacological inhibitors of ERK and p38 MAPKs, U0126 and SB203580, respectively (Fig. 1*A*). Although other effectors such as bacterial peptidoglycan have been reported to modulate PGE$_2$ release by activating COX-2 expression in a phosphatidylinositol 3-kinase-dependent manner, the phosphatidylinositol 3-kinase inhibitor wortmannin had no effect on PGE$_2$ release in the present instance. The ERK and p38 MAPKs appeared to regu-
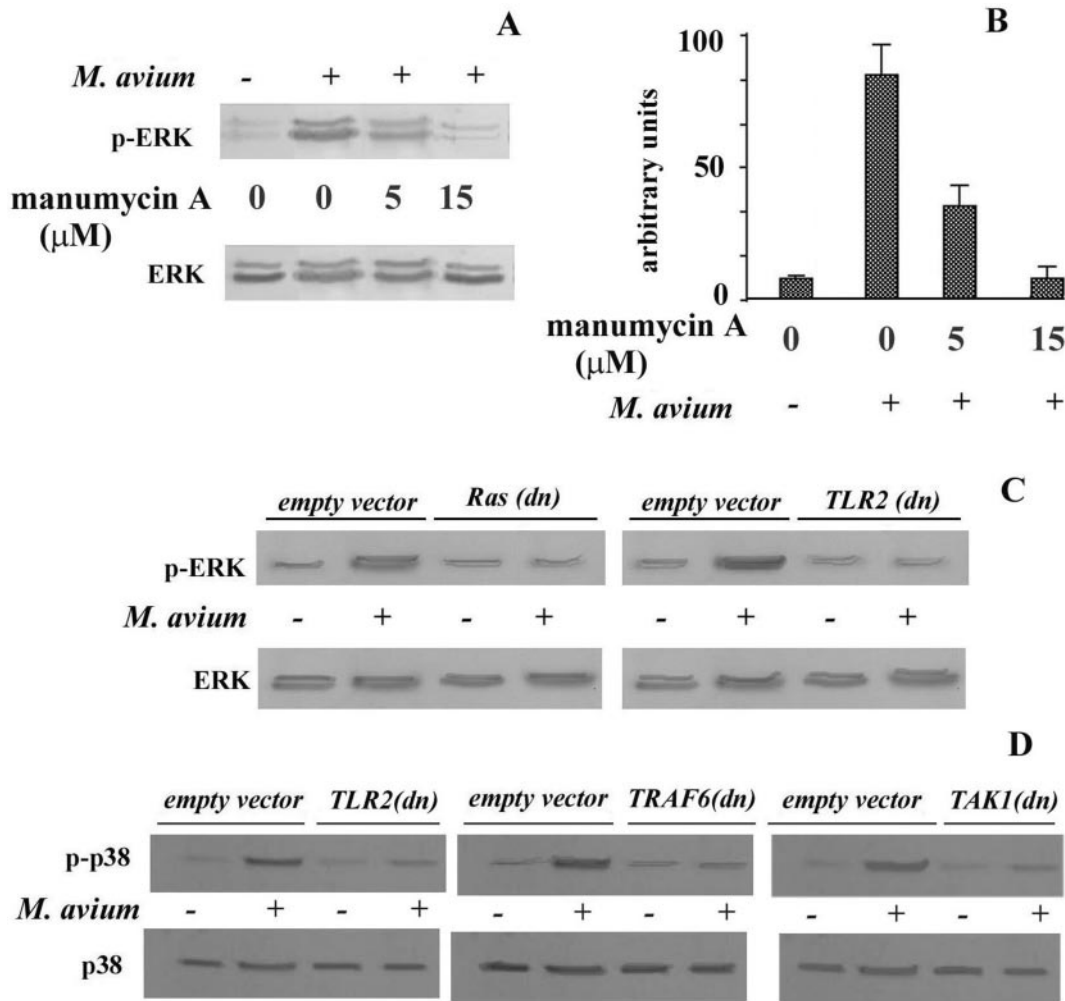
FIG. 3. ***M. avium*-dependent activation of ERK and p38 MAPKs.** *A*, RAW264.7 cells were left untreated or incubated with different concentrations of manumycin A for 30 min, followed by treatment with *M. avium* for 20 min. Cells were washed, lysed, and immunoblotted with phospho-ERK. All blots were reprobed with appropriate non-phospho antibodies to confirm equal loading. Blots shown are representative of results obtained in three independent experiments. The *bars* in *panel B* represent the results obtained by densitometric scans of three different blots corresponding to *panel B* (means ± S.D.). For *panels C* and *D*, RAW264.7 macrophages were transfected with empty vector (pcDNA3.1, pRK5, and pCMV for TLR2, TRAF6, and TAK1 constructs, respectively) or dominant-negative constructs followed by treatment with *M. avium* for 20 min. Cells were washed, lysed, and immunoblotted with phospho-ERK (*C*) or with phospho p38 (*D*) as described above.

late PGE$_2$ release in a synergistic manner, because a combination of the inhibitors U0126 and SB203580 led to a complete inhibition of PGE$_2$ release (Fig. 1*A*). Besides their ability to phosphorylate and activate transcription factors, both ERK and p38 MAPK also transduce signals by activating downstream kinases such as mitogen- and stress-activated protein kinase 1 (MSK1), which in turn phosphorylates transcription factors. Cells pretreated with H89, a pharmacological inhibitor of MSK1, at the dose used led to a complete inhibition of PGE$_2$ release (Fig. 1*A*), suggesting a role of MSK1 in PGE$_2$ release.

M. avium Stimulates COX-2 Expression—COX-2 converts arachidonic acid released from the cell lipids by the action of phospholipase A$_2$ to prostaglandin H2, the common precursor of all prostaglandins. To examine whether elevated PGE$_2$ synthesis is associated with increased COX-2 expression we studied the *M. avium*-induced expression of COX-2. Western analysis showed that *M. avium* challenge resulted in a time-dependent increase in the expression of COX-2 in RAW264.7 (Fig. 1*C*)

COX-2 expression is regulated by, among others, transcriptional mechanisms (7–12). We therefore analyzed the expression of the COX-2 gene in *M. avium*-challenged macrophages by reverse transcription-PCR. Compared with untreated cells,

the steady-state COX-2 mRNA levels increased in cells treated with *M. avium* (Fig. 1*E*). Taken together, our results on activation of COX-2 at the level of the gene and the protein in cells challenged with *M. avium* suggested that this regulation is likely to be critical in controlling PGE$_2$ release from these cells.

M. avium-induced COX-2 Expression Is Dependent on the MAPKs—Considering the role of MAPK inhibitors in inhibiting PGE$_2$ release, we tested the role of MAPKs in *M. avium*-induced COX-2 expression. As shown in Fig. 1 (*D* and *F*), *M. avium*-induced COX-2 expression could be attenuated partially either by U0126 or by SB203580 alone, suggesting a role of ERK as well as p38 MAPKs in *M. avium*-triggered COX-2 expression. As in the case of PGE$_2$ release, COX-2 expression was completely inhibited either by a combination of U0126 and SB203580, or by H89. The levels of COX-2 mRNA were also similarly regulated (Fig. 1*E*). These results suggested the possibility that COX-2 gene expression is coordinately regulated by ERK and p38 MAPKs regulating MSK1. This possibility has been tested in the following sections.

Ras Is Involved in M. avium-induced COX-2 Expression—The small GTP-binding protein Ras is an important signal mediator in response to stimuli such as growth factors, cytokines, and hormones (22). In resting cells, Ras is maintained in
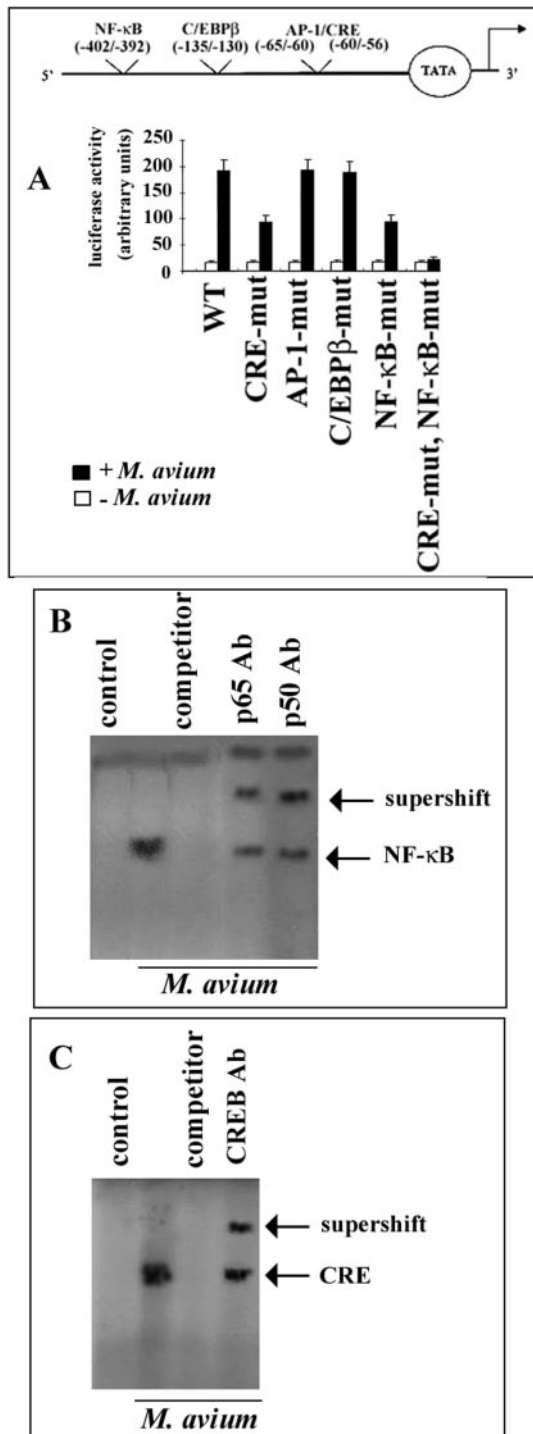
FIG. 4. ***M. avium*-stimulated COX-2 gene expression in RAW264.7 depends on the NF-κB and CRE elements of the COX-2 promoter.** *A*, cells were transfected with a COX-2 promoter-luciferase reporter construct or mutant constructs along with β-galactosidase expression vector. Transfected cells were either left untreated or treated with *M. avium* at an m.o.i. of 2 for 6 h. Luciferase reporter activities were measured in cell extracts using luciferin as a substrate. The level of induction of luciferase activity was compared with that of untreated cells. Data were normalized with respect to β-galactosidase activity. Results represent means ± S.D. of three independent experiments. *B* and *C*, electrophoretic mobility shift assays. RAW264.7 cells were left untreated or challenged with *M. avium* for 3.5 h. The nuclear extracts were subjected to EMSA using labeled COX-2-specific NF-κB (*B*) or CRE (*C*) DNA probes. Where required, the binding reaction was performed in the presence of competitor (unlabeled) oligonucleotides or supershift antibodies as indicated. The *arrowheads* indicate the position of bands. Gels are representative of results obtained from three independent experiments.

an inactivated Ras-GDP form. After activation, Ras is converted into active Ras-GTP. Ras exerts its function through activating downstream effectors, among which the best studied is the MAPK cascade (23). Considering the role of ERK and p38 MAPKs in regulating PGE_2 release as well as COX-2 expression in response to *M. avium* challenge, we tested the effect of the Ras inhibitor manumycin A (24) on *M. avium*-induced COX-2 expression. Cells were pretreated with manumycin A prior to challenge with *M. avium*. Manumycin A partially inhibited *M. avium*-induced COX-2 expression (Fig. 1, *D* and *F*). To further confirm the role of Ras in *M. avium*-induced signaling in RAW264.7 cells, the activation of Ras was assessed by an activation assay relying on the interaction of activated Ras with Raf-1-RBD (18). Upon *M. avium* challenge, Ras activity increased in a time-dependent manner (Fig. 2, *A* and *B*). Taken together, these results suggested that *M. avium*-induced COX-2 expression depends on Ras activation.

TLR2 Associates with Ras in M. avium-stimulated Macrophages—Because *M. avium*-mediated PGE_2 release is inhibited by dominant-negative TLR2, we tested the hypothesis that rapid Ras activation could be linked to TLR2 signaling. It was observed that *M. avium*-induced Ras activation was blocked in cells transfected with dominant-negative TLR2 (Fig. 2, *C* and *D*). To test whether rapid Ras activation is concurrent with Ras-TLR2 interaction, RAW264.7 cells were transfected with FLAG-tagged Ras and challenged with *M. avium*, and lysates were prepared and immunoprecipitated with anti-FLAG antibody and immunoblotted for the presence of TLR2 in the immunoprecipitated complex. The association of Ras and TLR2 occurred in a time-dependent manner (Fig. 2*E*). The immunoprecipitate showed no band corresponding to TLR2 when it was blotted with an irrelevant antibody. Control experiments were performed in which an irrelevant FLAG-tagged protein was transfected prior to challenge with *M. avium*. Co-immunoprecipitation of TLR2 with anti-FLAG antibody was not visible in this case. Taken together, all these results suggested that *M. avium*-induced Ras activation occurs through interaction of Ras with TLR2.

M. avium-induced ERK Activation Depends on TLR2/Ras Signaling—Our previous studies have already demonstrated that *M. avium* activates ERK and p38 MAPKs in macrophages (25). In the present study we observed that pretreatment with manumycin A (Fig. 3, *A* and *B*) inhibited the phosphorylation of ERK in a dose-dependent manner. This suggested that ERK was downstream of Ras signaling. Further, transfection of cells with dominant-negative TLR2 or dominant-negative Ras led to an inhibition of *M. avium*-induced ERK phosphorylation (Fig. 3*C*), supporting the view that *M. avium* activates ERK in a TLR2/Ras-dependent signaling pathway.

M. avium-induced p38 MAPK Activation Depends on TLR2/TRAF6 Signaling—*M. avium*-induced p38 MAPK activation was inhibited by transfecting cells with dominant-negative constructs of TLR2, TRAF6, or TAK1 (Fig. 3*D*). TAK1 is known to signal downstream of the TLRs to activate p38 MAPK in response to a variety of stimuli (26, 27). Because TLR2/TRAF6/TAK1 signaling is a well established pathway of MAPK activation, we felt it safe to predict that this pathway controls the activation of p38 MAPK in the present instance also.

M. avium Stimulates COX-2 Promoter Activity—COX-2 expression is controlled by both transcriptional and post-transcriptional mechanisms. To determine whether *M. avium* regulates COX-2 promoter activity, RAW 264.7 cells were transfected with different constructs of the mouse COX-2 promoter coupled with the luciferase reporter gene. *M. avium* evoked at least a 10-fold increase in luciferase activity in cells transiently expressing COX-2 promoter (−891 to + 9)-luc com-
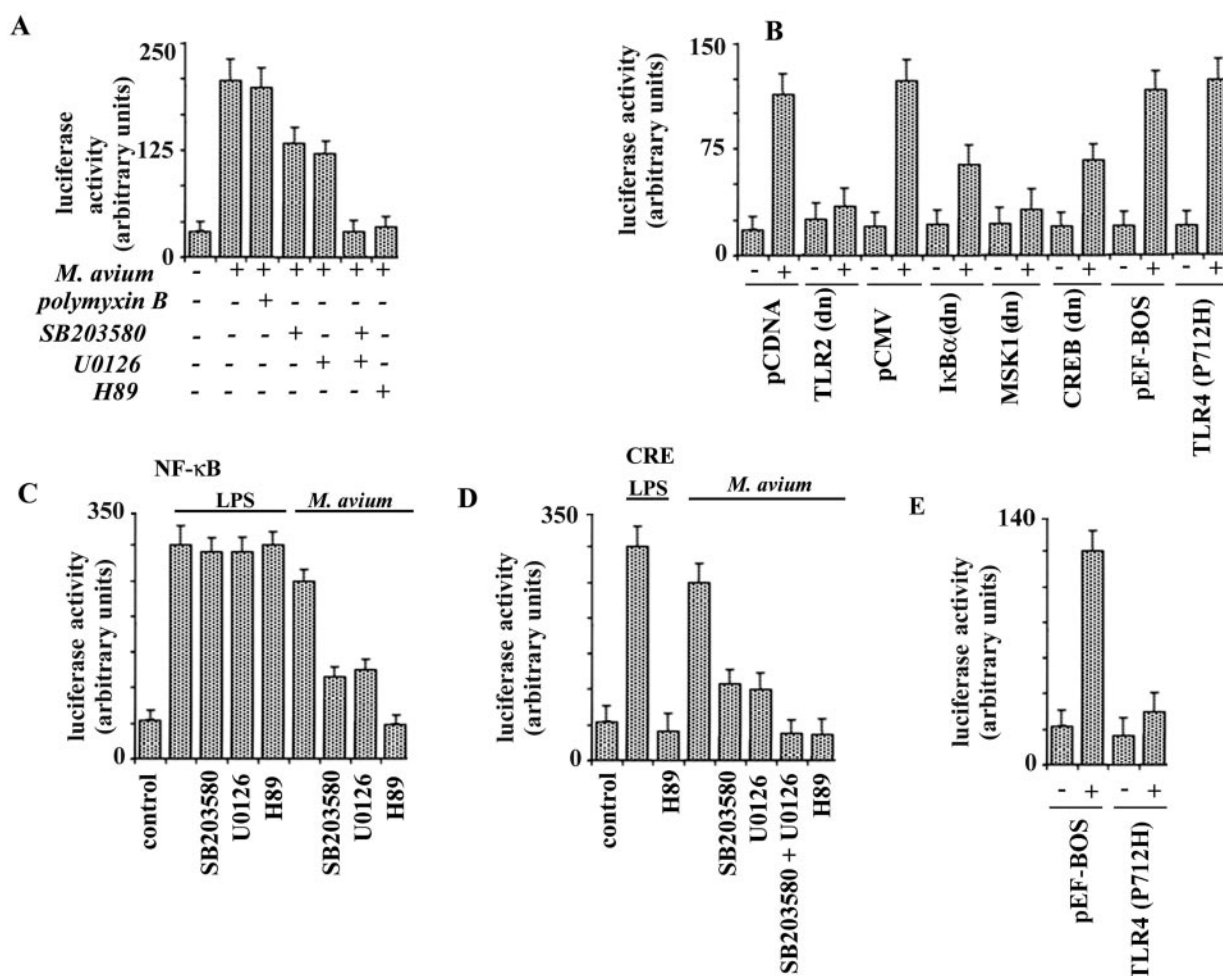
FIG. 5. ***M. avium* stimulates COX-2 promoter-driven luciferase reporter expression in RAW264.7.** RAW264.7 cells were transfected with the COX-2 promoter (−891 to +9)-luciferase reporter and β-galactosidase constructs. *A*, transfected cells were left untreated or treated with U0126 (15 μM), or SB203580 (5 μM), or H89 (10 μM), or a combination of U0126 and SB203580. Cells were then challenged for 6 h with *M. avium* or with *M. avium* preincubated with polymyxin B (10 μg/ml). In addition to the constructs mentioned above, cells were co-transfected (*B* and *E*) with empty vectors or constructs as indicated; followed by challenge with *M. avium* (*B*) or with *E. coli* LPS (*E*) for 6 h. *C* and *D*, cells were transfected with the 4× κB-luciferase construct (*C*) or the 6× CRE-luciferase construct (*D*) instead of the COX-2 promoter-luciferase construct. Transfected cells were treated with inhibitors (*C* and *D*) as described above. Cells were then left untreated or incubated with *E. coli* LPS or with *M. avium* (as indicated in the panels) for 6 h. Following incubations, luciferase reporter activities in the cell extracts were measured using luciferin as substrate. In each case, the level of induction of luciferase activity was compared with that of untreated cells. The activities shown represent data that have been normalized with β-galactosidase activity. Results represent the means ± S.D. of three independent experiments.

pared with untreated cultures (Fig. 4*A*). To rule out the effect of contaminating lipopolysaccharide (LPS) on COX-2 promoter-activated gene expression, *M. avium* cells were first incubated with polymyxin B before challenge of macrophages. The expression of luciferase was unchanged using polymyxin B-treated as compared with untreated *M. avium* (Fig. 5*A*).

The NF-κB and CRE Sites Are Essential for Optimal COX-2 Promoter-induced Reporter Induction in M. avium-stimulated Macrophages—In macrophages, several cis-acting elements have been found to play a role in COX-2 gene transcription (7–12). To assess the role of the potential cis-acting elements in *M. avium*-induced COX-2 gene transcription, the NF-κB, CRE, C/EBPβ, and AP-1 elements were individually mutated (as depicted in Fig. 4*A*) to evaluate the effects of such mutations on *M. avium*-stimulated COX-2 promoter activity. The COX-2 reporter constructs were transiently transfected into RAW264.7 macrophages. Cells were subsequently challenged with *M. avium* for 6 h, harvested, and lysed for luciferase activity reporter activity induced by *M. avium*. Our results demonstrate that the constructs mutated at the AP-1 and C/EBPβ sites were as effective in stimulating luciferase gene expression as the wild-type COX-2 promoter (Fig. 4*A*). However, there was

partial inhibition of luciferase gene expression when either the NF-κB or the CRE site was mutated, suggesting that *M. avium*-induced COX-2 promoter activation depends on the NF-κB as well as the CRE elements. Luciferase expression was completely inhibited when both the NF-κB and the CRE sites were mutated (Fig. 4*A*).

IκB-α Phosphorylation Is Necessary for M. avium-driven COX-2 Promoter Activation—In most cell types, NF-κB is maintained in an inactive form in the cytoplasm by association with IκBs. In the better known mechanisms of NF-κB activation, TLR signaling leads to the IκB kinase-dependent phosphorylation of IκB-α, its ubiquitination and degradation by the proteasome, accompanied by the release and subsequent translocation of NF-κB into the nucleus (28). The likely involvement of this classic pathway in *M. avium*-induced COX-2 promoter activation was tested. Transfection with dominant-negative TLR2 led to an inhibition of *M. avium*-stimulated luciferase activity (Fig. 5*B*). However, transfection with dominant-negative TLR4 (P712H) had no effect on *M. avium*-stimulated luciferase activity (Fig. 5*B*). The behavior of TLR4 (P712H) as dominant-negative was validated by the observation that this mutant could inhibit LPS-driven luciferase activation (Fig. 5*E*), corroborating the observa-

tions of Rhee and Hwang (29). Taken together, these results suggested that *M. avium*-mediated COX-2 gene expression is dependent on TLR2 but not on TLR4. The role of IκB-α phosphorylation was tested by transfecting cells with a mutated IκB-α(S32A/S36A) construct in which the two critical serine residues, which are phosphorylated by the IκB kinases, have been mutated; along with the COX-2 promoter-luciferase construct. Expression of the mutant IκBα protein partially blocked *M. avium*-dependent activation of the COX-2 luc reporter (Fig. 5*B*), indicating that the mutant IκBα protein was an effective repressor of COX-2 promoter-driven reporter expression. Considering that the phosphorylation and proteasome-mediated degradation of IκBα is the classic pathway of cytoplasmic NF-κB activation, the partial inhibition by pCMV-IκB-α(S32A/S36A) was expected and supported by our observations that transfection with the mutant IκB-α(S32A/S36A) construct inhibited *M. avium*-induced 4x κB-driven luciferase expression (Fig. 5*E*). Canonical NF-κB activation was therefore required for *M. avium*-induced COX-2 reporter activity.

There are results both in favor and against a role of NF-κB in the stimulation of COX-2 gene expression. Whereas, NF-κB activates a COX-2 promoter construct in IL-1β-stimulated pulmonary type II A549 cells (30), it plays no role in COX-2 induction in tumor necrosis factor-α-stimulated rat vascular smooth muscle cells (31). Our present studies definitively show that *M. avium*-stimulated gene expression driven by the COX-2 promoter depends on the NF-κB element on the COX-2 promoter.

We also examined whether the NF-κB activation correlates with differences in NF-κB-specific DNA binding. Nuclear extracts were prepared from untreated cells as well as cells treated for 3.5 h with *M. avium*. Extracts from *M. avium*-treated cells showed binding to an oligonucleotide sequence corresponding to the NF-κB-binding site of the COX-2 promoter (Fig. 4*B*), and DNA binding was inhibited by excess unlabeled oligonucleotide. No binding was observed when a mutant NF-κB-binding oligonucleotide sequence was used (data not shown). Supershift of the band obtained with the NF-κB-specific oligonucleotide with anti-p65 or anti-p50 (Fig. 4*B*) suggested that p65 and p50 are the components of the protein complex that binds to the NF-κB element of the COX-2 promoter.

The MAPKs ERK and p38 Regulate M. avium-induced COX-2 Promoter Activation—To analyze the effect of ERK and p38 MAPK activation on COX-2 promoter-driven luciferase expression in *M. avium*-challenged RAW264.7, cells were pretreated with ERK and p38 MAPK-specific inhibitors U0126 and SB203580, respectively. Both these inhibitors caused a partial inhibition of luciferase expression (Fig. 5*A*). However, a combination of both inhibitors completely inhibited luciferase expression, suggesting that ERK and p38 MAPK activation are critical in sustaining *M. avium*-driven COX-2 promoter activation.

MSK1 Is Activated in M. avium-stimulated Macrophages—The MAPKs phosphorylate several downstream kinases, one of which is MSK1, which is constitutively localized in the nucleus where it regulates transcription by phosphorylating histone H3, p65/RelA, and CBP/p300 (32, 33) leading to modification of nucleosome conformation and increased accessibility of the transcription machinery to promoters. ERK and p38 are both known to activate MSK1 (34). To determine whether the effects of ERK and p38 MAPKs are transmitted through the activation of MSK1, we first investigated the ability of *M. avium* to trigger the activation of MSK1. MSK1 kinase activity was determined in *M. avium*-treated macrophages by immunoprecipitating MSK1 from cell lysates and assaying the ability of the immunoprecipitates to phosphorylate the peptide: EILSRRPSYRK
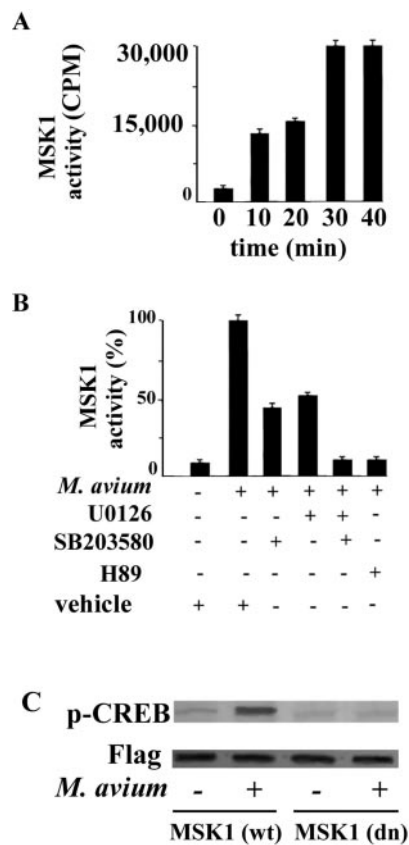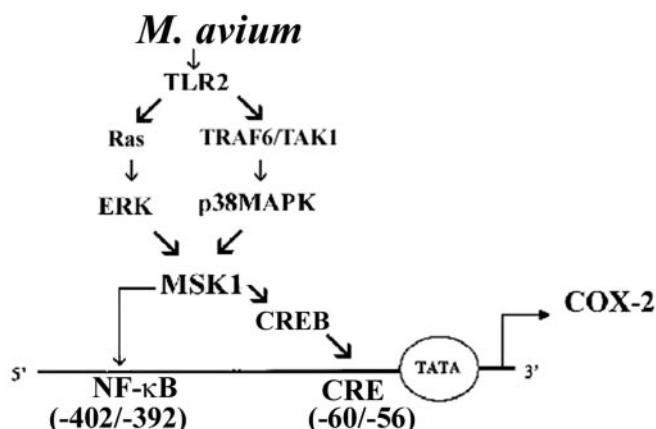

FIG. 6. ***M. avium*-stimulated MSK1 regulates CREB phosphorylation in RAW264.7 macrophages.** *A*, cells were left untreated or treated with *M. avium* for different periods of time. Cell lysates were immunoprecipitated with MSK1 antibody, and the immunoprecipitate was used to measure the phosphorylation of the substrate CREB-tide as described under "Experimental Procedures." *B*, cells were incubated without or with the indicated inhibitors for 30 min followed by treatment with *M. avium* for 30 min. Cell lysates were used to measure MSK1 activity as described above. Data have been represented as values relative to that obtained in cells treated with *M. avium* (100%). Results in *A* and *B* are the means ± S.D. of three independent experiments. *C*, cells were transfected with wild type FLAG-MSK1 or dominant-negative MSK1 (*MSK1(dn)*) followed by challenge with *M. avium* for 30 min. Lysates were prepared, separated on SDS-PAGE, and blotted with anti-phospho-CREB antibody. The *bottom panel* is a blot using anti-FLAG antibody to show equal loading. The blot shown is representative of the results obtained in three independent experiments.

(CREBTIDE) (34). *M avium* activated MSK1 in a time-dependent manner (Fig. 6*A*). MSK1 activity could be partially inhibited by pretreatment with either U0126 or SB203580 (Fig. 6*B*), suggesting a role of both ERK and p38 MAPK signaling in MSK1 activation. A combination of U0126 and SB203580 completely blocked MSK1 activation (Fig. 6*B*), suggesting that ERK and p38 MAPK act synergistically to activate MSK1. The finding that both kinases are required for MSK1 activity raises the possibility that they may phosphorylate non-overlapping sites that affect the kinase activity of MSK1, or that the two kinases regulate each other, or that the activity of neither of the two kinases is sufficient to fully phosphorylate MSK1. Whatever the mechanism, our findings suggest that MSK1 plays an essential role functioning as a downstream effector of *M. avium* signaling controlling both NF-κB- and CRE-driven COX-2 promoter activation. The following sections detail our attempts to address this question.

CREB Plays a Role in M. avium-induced COX-2 Promoter Activation—CREB, a member of the ATF family of transcription factors, binds to the CRE element. Because mutation of the COX-2 CRE site inhibits COX-2 reporter activity, we explored

Fig. 7. **Model depicting the *M. avium*-triggered signaling pathways regulating COX-2 gene expression.**

the role of CREB in *M. avium*-induced COX-2 reporter activity. Transfection of cells with dominant-negative CREB along with the COX-2-luciferase construct led to an inhibition of *M. avium*-driven COX-2 promoter activity (Fig. 5*B*).

CREB Is Phosphorylated in M. avium-stimulated Macrophages—CREB is a target of MSK1 (35). We examined whether CREB phosphorylation is differentially regulated in untreated and *M. avium*-challenged macrophages and whether MSK1 regulates this process. To test this, cells were transfected with wild type or dominant-negative MSK1 and challenged with *M. avium*. Lysates from *M. avium*-challenged and untreated macrophages were probed with an antibody that specifically recognizes CREB phosphorylated at Ser-133. Our results showed that CREB phosphorylation was enhanced in *M. avium*-challenged macrophages and that this was abrogated in cells transfected with dominant-negative MSK1 (Fig. 6*C*).

We also examined whether the enhanced CREB phosphorylation correlated with differences in CREB-specific DNA binding. Nuclear extracts were prepared from untreated cells as well as cells treated for 3.5 h with *M. avium*. Only extracts from *M. avium*-treated cells showed binding to an oligonucleotide sequence corresponding to the CREB-binding site of the COX-2 promoter (Fig. 4*C*). DNA binding was inhibited by excess unlabeled oligonucleotide. No binding was observed when a mutant CREB-binding oligonucleotide sequence was used (data not shown). Anti-CREB antibody supershifted the band obtained with the CREB-specific DNA probe suggesting that CREB binds to the CRE element of the COX-2 promoter.

MSK1 Is Necessary For Regulating COX-2 Promoter-driven Gene Expression in M. avium-challenged Macrophages—To assess the effects of MSK1 on COX-2-promoter-driven luciferase expression in *M. avium*-treated macrophages, cells pretreated with H89 (Fig. 5*A*) or transfected with dominant-negative MSK1 (Fig. 5*B*) were subsequently challenged with *M. avium*, and luciferase gene expression was assayed. In each case, suppression of MSK1 activity led to almost complete inhibition of luciferase expression, suggesting that MSK1 plays an important role in regulating activation of the COX-2 promoter following *M. avium* challenge. We further analyzed the role of *M. avium*-mediated MSK1 activation on NF-κB and CRE-driven luciferase expression by transfecting cells with a luciferase reporter gene fused downstream of either a 4× κB element or a 6× CRE element. *M. avium* could activate both NF-κB-driven (Fig. 5*C*) and CRE-driven (Fig. 5*D*) luciferase expression in these cells. However, such activation was abrogated in cells in which MSK1 activity was inhibited by treatment with H89. Transfection with dominant-negative MSK1 gave similar results (data not shown). These results definitively demonstrated that MSK1 regulates both NF-κB- and CRE-driven gene expression triggered by *M. avium*. In this

regard, the effect of *M. avium* was different from that observed in the case of LPS. We observed that *Escherichia coli* LPS-stimulated NF-κB- and CRE-driven luciferase expression (Fig. 5, *C* and *D*). The latter effect could be inhibited in cells pretreated with H89 (Fig. 5*D*). However, NF-κB- driven luciferase expression could not be inhibited by pretreatment with U0126 or SB203580 or H89 (Fig. 5*C*).

DISCUSSION

High PGE$_2$ concentrations during mycobacterial infection cause down-regulation of cell-mediated immunity permitting disease progression (36). The immunosuppressive effects of prostaglandin E$_2$ in relation to mycobacterial infection underscore the need to understand the mechanisms regulating the expression of the rate-limiting enzyme in prostaglandin synthesis, COX-2. Animal models of tuberculosis have demonstrated that blocking of COX-2 produced high inflammation and expression of tumor necrosis factor-α and interferon-γ. Although previous reports have shown that virulent *M. avium* stimulates the expression of COX-2, the signaling pathways regulating COX-2 expression remain to be studied. The data presented in this report focus on the role of signaling pathways in *M. avium*-induced COX-2 gene transcription. Our data demonstrate that *M. avium*-induced gene expression driven by the COX-2 promoter depends on TLR2-dependent signaling converging on the NF-κB and CRE-elements present in the promoter, but not on the C/EBPβ or the AP-1 elements. Mutation at either the NF-κB-binding site or at the CRE-binding site led to a partial inhibition of *M. avium*-induced COX-2 promoter-driven luciferase gene expression (Fig. 4*A*), whereas mutation at both these sites completely inhibited luciferase expression. At the same time, nuclear extracts from *M. avium*-challenged macrophages effected electrophoretic mobility shifts of oligonucleotides corresponding to the COX-2-gene specific NF-κB and CRE sites (Fig. 4, *B* and *C*). Transcription factor NF-κB has been shown to induce macrophage COX-2 in response to a variety of stimuli (37). Rhee and Hwang (29) have demonstrated that LPS triggers TLR4-mediated NF-κB activation leading to COX-2 gene expression. Our studies demonstrate that TLR2 contributes to *M. avium*-induced COX-2 gene induction (Fig. 5). Suppressor IκB-α transfection led to inhibition of COX-2 promoter activity as well as consensus NF-κB-driven promoter activity (Fig. 5, *B* and *E*). These results supported a role of the canonical NF-κB activation in *M. avium*-stimulated COX-2 promoter activation. *M. avium*-induced canonical NF-κB activation was also observed by Giri *et al.* (38). In addition to the classic pathway, TLRs are known to activate downstream signaling cascades through small G proteins such as Rac and Ras to mediate NF-κB activation. We observed that *M. avium* challenge led to association of Ras with TLR2 and a

Mycobacteria-induced COX-2 Expression in Macrophages

rapid activation of Ras (Fig. 2). COX-2 promoter activation, as well as activation of the consensus NF-κB promoter relied on TLR2/Ras-dependent ERK activation (Fig. 3*A*). In the classic Toll signaling pathway, TLRs upon recognizing suitable ligands recruit MyD88/IRAK/TRAF6. This leads to the activation of MAPK kinase kinases such as TAK1. *M. avium* triggered TLR2/TRAF6/TAK1-dependent p38 MAPK activation (Fig. 3*D*). Both ERK and p38 MAPK were responsible for the activation of the nuclear kinase MSK1. A combination of pharmacological inhibitors of ERK and p38 completely inhibited MSK1 activation (Fig. 6*B*). Inhibitors of either ERK or p38 (U0126 or SB203580, respectively) partially inhibited NF-κB-driven luciferase expression, whereas H89 could block luciferase expression completely (Fig. 5*C*). These results clearly demonstrated that MSK1 plays an important role in *M. avium*-triggered NF-κB activation. This effect of *M. avium* on RAW264.7 macrophages was different from that reported in the case of LPS-driven COX-2 expression in RAW264.7, where LPS-driven NF-κB activation has been shown to occur independent of ERK (39) or MSK1 (8) activation. Previous work by Deak *et al.* (34) demonstrated that the transcription factors CREB and ATF1 are physiological substrates of MSK1. In the present study we also observed that *M. avium* induced phosphorylation of CREB in an MSK1-dependent manner (Fig. 6*C*).

In summary, *M. avium* triggers TLR2-dependent signaling leading to the phosphorylation of ERK and p38 MAPKs, which converge to activate MSK 1 (Fig. 7). MSK1 regulates both the NF-κB- and the CRE-driven gene transcription. Both phosphorylated CREB and NF-κB are known to recruit histone acetylases such as CBP/p300, which in turn contribute to making the promoter more accessible to transcription factors and help in bridging the transcription factor-CBP complexes to components of the basal transcription machinery (40). MSK1 phosphorylates histone H3 (41) and has also been identified as a nuclear kinase for p65, phosphorylating p65 at serine 276 (42). Our results point to the fact that MSK1-dependent changes, likely at the level of the nucleosome, are prerequisite for *M. avium*-driven COX-2 gene expression. The nature of nucleosome remodeling following *M. avium* infection is presently under investigation.

REFERENCES

1. Chouaib, S., Welte, K., Mertelsmann, R., and Dupont, B. (1985) *J. Immunol.* **135,** 1172–1179
2. Hasler, F., Bluestein, H. G., Zvaifler, N. J., and Epstein, L. B. (1983) *J. Immunol.* **131,** 768–772
3. Tse, H. M., Josephy, S. I., Chan, E. D., Fouts, D., and Cooper, A. M. (2002) *J. Immunol.* **168,** 825–833
4. Ridgway, D., Wolff, L., Wall, M., Borzy, M., and Kirkpatrick, C. (1991) *J. Clin. Immunol.* **11,** 357–362
5. Denis, M. (1994) *Clin. Exp. Immunol.* **98,** 123–127
6. Herschman, H. R. (1996) *Biochim. Biophys. Acta* **1299,** 125–140
7. Smith, W. L., DeWitt, D. L., and Garavito, R. M. (2000) *Annu. Rev. Biochem.* **69,** 145–182
8. Caivano, M., and Cohen, P. (2000) *J. Immunol.* **164,** 3018–3025
9. Chen, J. D., Patriotis, C. P., Tsatsanis, C., Makris, A. M., Kovatch, R., Swing, D. A., Jenkins, N. A., Tsichlis, P. N., and Copeland, N. G. (1997) *Mol. Pharmacol.* **59,** 493–500
10. Wadleigh, D. J., Reddy, S. T., Kopp, E., Ghosh, S., and Herschman, H. R. (2000) *J. Biol. Chem.* **275,** 6259–6266
11. Caivano, M., Gorgoni, B., Cohen, P., and Poli, V., (2001) *J. Biol. Chem.* **276,** 48693–48701
12. Iniguez, M. A., Martinez-Martinez, S., Punzon, C., Redondo, J. M., and Fresno, M. (2000) *J. Biol. Chem.* **275,** 23627–23635
13. Thomas, B., Berenbaum, F., Humbert, L., Bian, H., Bereziat, G., Crofford, L., and Olivier, J. L. (2000) *Eur. J. Biochem.* **267,** 6798–6809
14. Inoue, H., Yokoyama, C., Hara, S., Tone, Y., and Tanabe, T. (1995) *J. Biol. Chem.* **270,** 24965–24971
15. Subbaramaiah, K., Chung, W. J., Michaluart, P., Telang, N., Tanabe, T., Inoue, H., Jang, M., Pezzuto, J. M., and Dannenberg, A. J. (1998) *J. Biol. Chem.* **273,** 21875–21882
16. Xie, W., and Herschman, H. R. (1995) *J. Biol. Chem.* **270,** 27622–27628
17. Morris, J. K., and Richards, J. S. (1996) *J. Biol. Chem.* **271,** 16633–16643
18. Taylor, S. J., Resnick, R. J., and Shalloway, D. (2001) *Methods Enzymol.* **333,** 333–342
19. Alessi, D. R., Cohen, P., Ashworth A., Cowley, S., Leever, S. J., and Marshall, C. J. (1995) *Methods Enzymol.* **255,** 279–290
20. Basu, J. (2004) *Curr. Sci.* **86,** 103–110
21. Lien, E., Sellati, T. J., Yoshimura, A., Flo, T. H., Rawadi, G., Finberg, R. W., Carroll, J. D., Espevik, T., Ingalls, R. R., Radolf, J. D., and Golenbock, D. T. (1999) *J. Biol. Chem.* **274,** 33419–33425
22. Wittinghofer, F. (1998) Nature **394,** 319–320
23. Marshall, C. J. (1996) *Curr. Opin. Cell Biol.* **8,** 197–204
24. Hara, M., and Han, M. (1995) *Proc. Natl. Acad. Sci. U. S. A.* **92,** 21096–21103
25. Bhattacharyya, A., Pathak, S., Kundu, M., and Basu, J. (2002) *FEMS Immunol. Med. Microbiol.* **34,** 73–80
26. Muzio, M., Polentarutti, N., Bosisio, D., Manoj Kumar, P. P., and Manotvani, A. (2000) *Biochem. Soc. Trans.* **28,** 563–566
27. Ge, B., Gram, H., Di Padova, F., Huang, B., New, L., Ulevitch, R. J., Luo, Y., and Han, J. (2002) *Science* **295,** 1291–1294
28. Ghosh, S., May, M. J., and Kopp, E. B. (1998) *Annu. Rev. Immunol.* **16,** 225–260
29. Rhee, S. H., and Hwang, D. (2000) *J. Biol. Chem.* **275,** 34035–34040
30. Newton, R., Kuitert, L. M. E., Bergmann, M., Adcock, I. M., and Barnes, P. J. (1997) *Biochem. Biophys. Res. Commun.* **237,** 28–32
31. Chen, G., Wood, E. G., Wang, S. H., and Arner, T. D. (1999) *Life Sci.* **64,** 1231–1242
32. Davie, J. R. (2003) *Science's STKE* http://stke.sciencemag.org/cgi/content/full/sigtrans;2003/195/pE33
33. Janknecht, R. (2003) *Oncogene* **22,** 746–755
34. Deak, M., Clifton, A. D., Lucocq, L. M., and Alessi, D. R. (1998) *EMBO J.* **17,** 4426–4441
35. Arthur, J. S. C., and Cohen, P. (2000) *FEBS Lett.* **482,** 44–48
36. Rangel, M. J., Estrada, G. I., De La Luz, G. H. M., Aguilar L. D., Marquez, R., and Hernandez, P. R. (2002) *Immunology* **106,** 257–266
37. Baeuerle, P. A., and Henkel, T. (1994) *Annu. Rev. Immunol.* **12,** 141–179
38. Giri, D. K., Mehta, R. T., Kansal, R. G., and Aggarwal, B. B. (1998) *J. Immunol.* **161,** 4834–4841
39. Chen, C.-C., and Wang, J.-K. (1999) *Mol. Pharmacol.* **55,** 481–488
40. Sheppard, K.-A., Rose, D. W., Haque, Z. K., Kurokawa, R., McInerney, E., Westin, S., Thanos, D., Rosenfeld, M. G., Glass, C. K., and Collins, T. (1999) *Mol. Cell Biol.* **19,** 6367–6378
41. Thomson, S., Clayton, A. L., Hazzalin, C. A., Rose, S., Barratt, M. J., and Mahadevan, L. C. (1999) *EMBO J.* **18,** 4779–4793
42. Vermeulen, L., De Wilde, G., Van Damme, P., Vanden Berghe, W., and Haegeman, G. (2003) *EMBO J.* **22,** 1313–1324